

TRANSIENT STABILITY IMPROVEMENT OF POWER SYSTEM USING SMES BASED FAULT CURRENT LIMITER

M. Jafari¹ M.R. Alizadeh Pahlavani²

1. Faculty of Electrical and Computer Engineering, University of Tabriz, Tabriz, Iran, m.jafari87@ms.tabrizu.ac.ir
2. Malek Ashtar University of Technology, Tehran, Iran, mr_alizadehp@iust.ac.ir

Abstract- In this paper, transient stability improvement using Superconducting Magnetic Energy Storage based Fault Current Limiter (SMES-based FCL) is presented. The proposed SMES-based FCL is installed at the beginning of faulty line. The proposed SMES-based FCL inserts a superconducting inductance into the fault current pass. The insertion of high value of inductance not only limits the fault current level in an acceptable level but also improves transient stability of power system by storing excessive energy of synchronous generators during the fault. Moreover, the proposed FCL can improve the voltage profile during short circuit faults. Analytical analysis of the FCL's performance are presented in detail and simulation results in the IEEE standard 14-bus system using EMTDC/PSCAD software are included to show the current limiting feature, voltage sag prevention and transient stability enhancement using the proposed SMES-based FCL.

Keywords: Fault Current Limiter, SMES Magnet, Transient Stability Improvement, Voltage Profile.

I. INTRODUCTION

Nowadays, due to considerable increase in electric power demand, power systems have become more complicated. To support power demand, modern systems must be connected each other. In addition, green resource energies and different types of distributed generation such as solar energy and wind energy have been introduced. This may increase power flow and short circuit capacity of the power networks. So, occurring a short circuit fault in the power lines results in very high-level fault currents, which flow in the power system series equipment and may damage them [1-4].

Using fault current limiter (FCL) is a promising way to overcome the high-level short circuit currents and prevent the high costs of switchgear replacement in power systems [5-8]. Solid state, superconducting (resistive type and inductive type) and resonance type FCLs have been presented in [7] to [11]. Using a superconducting DC reactor in solid state fault current limiter reduces increasing rate of fault current until the operation of circuit breakers. During fault current limiting mode, active power is absorbed by superconducting DC reactor.

To reach better limitation of such FCLs, large value of DC reactor must be taken into account. Low power losses and no need to quenching characteristics of superconductors are main advantages of the mentioned FCL [12, 13]. By increasing the value of inductance in inductive type superconductor, stored electrical energy can be increased. This is the main idea of superconducting magnetic energy storage (SMES). Ferrier has presented SMES technology in 1969. However, more studies on this field illustrated that the SMES has better performance in power system operating applications than the energy storage application [14-18].

One of the applications of SMES technology is using its superconducting reactor in FCL structure [19, 20]. SMES technology can produce DC reactor with large value, which is needed in solid state FCLs. Such reactor will have large value and low losses due to its superconducting characteristic. Main applications of FCLs in addition to limiting the fault current are transient stability enhancement of the power system, power quality and reliability improvement [1, 20, 21]. Increasing power flow in the power lines due to increasing power demand can affect the stability of the power system especially during large disturbances such as short circuit faults.

Most of studies on this issue have focused on superconducting FCLs (SFCLs) which operate by quenching of superconductor. Base of all of these structures is to limit the fault current, restore the bus voltage, and absorb active power of generators during the fault. This action can help the generator to maintain its stability. Therefore, transient stability of power system will be improved in short circuit conditions [20-26].

However, these FCL structures have two main problems. Firstly, they make the superconductor to change from superconducting state to normal state and vice versa, which leads to power losses. Secondly, they have recovery time due to quenching phenomenon. Recovery time leads to more time required by FCL to retreat from the power system and this makes disturbance in voltage profile. In this paper, a SMES-based FCL is applied to enhancement of IEEE standard 14-bus power system's transient stability. Maximum oscillation of angular frequency of all generators has been considered as a criterion to show the effectiveness of the proposed structure.

It is observed that using SMES technology can help the limiting characteristics of FCL and improves the transient stability of system. In addition, this FCL can help to improve voltage profile in fault condition. Average voltage sag on system buses during the fault is measured to show this capability of proposed FCL. Such structure has not recovery time and has low power losses in comparison with the other structures, which are used for this purpose.

The analytical analysis for FCL operation and transient stability analysis are presented in detail. simulation study on IEEE standard 14-bus power system including the proposed FCL is established using EMTDC/PSCAD software. Results are discussed carefully to show the performance of the proposed FCL on the transient stability improvement.

II. POWER CIRCUIT TOPOLOGY AND PRINCIPLES OF OPERATION

A. Power Circuit Topology

The three-phase power circuit topology of the proposed FCL is shown in Figure 1. This structure is composed of three main parts, which are described as follows:

- 1- The three-phase transformer in series with the system that is named "Isolation transformer"
- 2- The three-phase diode rectifier bridge
- 3- A SMES magnet as DC reactor with large value

As a conventional method, isolation transformer is needed to direct the line current to current limiting part. Three-phase diode bridge is AC/DC converting tool for FCL and SMES magnet is the main part of FCL which has the current limiting task during the short circuit fault.

B. Principles of Operation

In normal operation of power system, diode bridge rectifies line current to DC current and this DC current charges SMES magnet. When the DC current reaches to the peak of line current, SMES magnet behaves as short circuit because of its superconducting characteristic and so, voltage drop on it becomes almost zero. Very small voltage drop on SMES magnet is due to DC current ripple. By this way, total voltage drop on FCL will be related to voltage drop on diodes and isolation transformer, which is negligible in comparison with feeder's nominal voltage.

Therefore, FCL has not considerable effect on the normal operation of power system. As fault occurs, line current starts to increase. However, the SMES magnet limits its increasing rate and prevents fault current rapid increment. In this case, fault energy will be stored in SMES magnet. Since the value of SMES magnet is large, this current limitation is in acceptable range, which will be shown in simulation results. By this manner, the voltage of connected bus does not experience considerable sag in comparison with the case of no FCL.

Therefore, power flow in system will be not interrupted by the fault and transient stability of system will be improved. By removal of the fault, system returns to its normal state and SMES magnet starts to discharge. Since the SMES magnet is in its superconducting state during the fault and has not quenching phenomenon, there will not be any recovery time and so, just after fault removal, FCL retreats from the system.

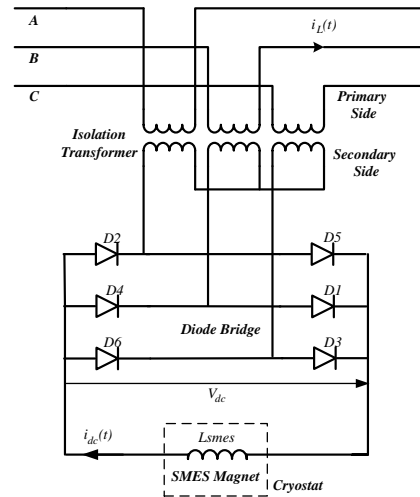


Figure 1. Three-phase power circuit topology of the proposed FCL

III. ANALYTICAL ANALYSIS OF THE PROPOSED FCL

This section deals with the analytical analysis of the proposed FCL's performance in current limiting during the fault. To calculate the equation of line current and DC current, two modes are considered as Pre-Fault Condition, and Fault Duration.

A. Pre-Fault Condition

In pre-fault condition, line current, $i_L(t)$, and DC current, $i_{dc}(t)$ have two modes as Charging mode and Discharging mode. DC current and diodes currents are shown in Figure 2. Enlarged view of these currents is shown in Figure 3. Charging mode begins at t_0 and ends at t_1 . In this mode, one diode from each phase is ON. So, the following equation can be written.

$$V_m \sin(\omega t) = ri(t) + L \frac{di(t)}{dt} + V_D \quad (1)$$

where, $i = i_{dc} = i_L$, $r = r_s + r_{FCL} + r_L$, $L = L_s + L_{SMES} + L_L$, r_s and L_s are source side's resistor and inductor, respectively, r_L and L_L are load side's resistor and inductor, respectively, r_{FCL} is equivalent resistance of FCL's elements and V_D is voltage drop on each diode. Solving Equation (1) leads to:

$$i(t) = e^{-\frac{r}{L}(t-t_0)} \left(I_0 - \frac{V_m}{z} \sin(\omega t_0 - \varphi) + \frac{V_D}{r} \right) + \frac{V_m}{z} \sin(\omega t - \varphi) - \frac{V_D}{r} \quad (2)$$

where, $I_0 = i(t_0)$, $z = \sqrt{r^2 + (L\omega)^2}$, $\varphi = \tan^{-1}(L\omega/r)$.

Discharging mode starts at t_1 and continues to t_2 . In this mode, both diodes of each phase are ON and therefore the line current is sinusoidal waveform and FCL behaves as a series transformer with short-circuited secondary. In such condition, DC current differential equation can be derived as follow:

$$L_{SMES} \frac{di_{dc}}{dt} + r_D i_{dc} + 2V_D = 0 \quad (3)$$

where, r_D is the diode's resistance. Note that its value is very small. By solving Equation (3), DC current formula will be as follow:

$$i_{dc}(t) = e^{-\frac{r_D}{L_{SMES}}(t-t_1)} (I_{max} + 2V_D / r_D) - 2V_D / r_D \quad (4)$$

Considering charging and discharging modes of current, it is possible to calculate the average value (I_{dc}) and ripple (i_r) of DC current. As it is obvious, DC current's ripple leads to voltage drop on SMES magnet and therefore on FCL. For I_{dc} and i_r , we can write:

$$I_{dc} = I_{max} - \frac{i_r}{2} \quad (5)$$

$$i_r = \frac{1}{2}(I_{max} - I_0) \quad (6)$$

where, I_{max} is the peak of line current. I_0 in Equation (6) can be calculated from Equation (4) in t_2 instant as follow:

$$I_0 = e^{-\frac{r_D}{L_{SMES}}(t_2-t_1)} (I_{max} + \frac{2V_D}{r_D}) - \frac{2V_D}{r_D} \quad (7)$$

By considering that $e^{-x} \approx (1-x)$ and $t_2 - t_0 = T / 6$, where T is the time period of power system, Equation (7) can be simplified to Equation (8).

$$I_0 = (1 - r_D T / 9 L_{SMES}) (I_{max} + \frac{2V_D}{r_D}) - \frac{2V_D}{r_D} \quad (8)$$

Therefore, i_r can be derived from combination of Equations (6) and (8).

$$i_r = (\frac{2Tr_D}{L_{SMES}})(I_{max} + \frac{2V_D}{r_D}) \quad (9)$$

It is important to note that its value is very small due to very small value of r_D / L_{SMES} . Considering Equation (9), the voltage drop on SMES magnet can be calculated as Equation (10).

$$V_{SMES} = 24 \frac{r_D}{L_{SMES}} (I_{max} + \frac{2V_D}{r_D}) \quad (10)$$

By using Equation (9), formula of I_{dc} can be written as follow:

$$I_{dc} = I_{max} (1 - \frac{Tr_D}{L_{SMES}}) - \frac{2TV_D}{L_{SMES}} \quad (11)$$

It is obvious that the average of SMES magnet's current is very close to the peak of line current. This value can be used for designing the SMES magnet.

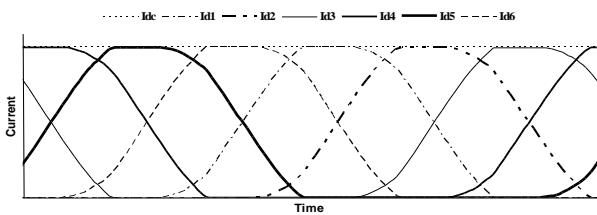


Figure 2. DC current and diodes currents in the normal operation of power system

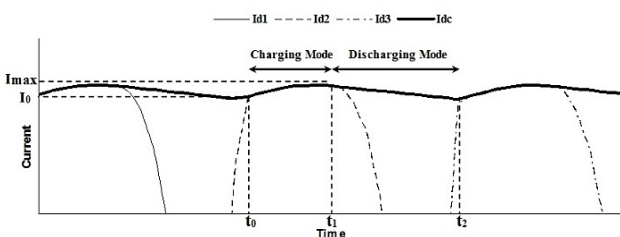


Figure 3. Enlarged view of Figure 2

B. Fault Duration

Considering Figure 4, fault occurs at t_f . The fault condition has two modes as M_1 and M_2 . The mode M_1 is in t_3 to t_4 time interval and in this mode, diodes D_4 and D_5 are ON, while D_1, D_2, D_3 and D_6 are OFF. Therefore, current of phase B is equal to negative value of current of phase A and current of phase C is zero (Figure 5). The zero sections, which are appeared in the line current, are due to the commutation of diodes. In the normal operation, commutation of diodes was based on their current, while, in the fault condition, there will be voltage commutation on diodes. In such condition, formula of current of phase A can be written as follow:

$$V_m \sin(\omega t) = r i_A(t) + L \frac{di_A(t)}{dt} + V_D \quad (12)$$

$$i_A(t) = e^{-\frac{r}{L}(t-t_3)} (I_3 - \frac{V_m}{z} \sin(\omega t_3 - \varphi) + \frac{V_D}{r}) + \frac{V_m}{z} \sin(\omega t - \varphi) - \frac{V_D}{r} \quad (13)$$

where, $r = r_s + r_{FCL}$, $L = L_s + L_{smes}$, $z = \sqrt{r^2 + (L\omega)^2}$, $\varphi = \tan^{-1}(L\omega / r)$ and $I_3 = i_A(t_3)$.

Note that the DC current relation is same as current of phase A in this mode. For phase B and C , as pointed previously, $i_B(t) = -i_A(t)$ and $i_C(t) = 0$. In mode M_2 , Diodes D_4 and D_1 are in commutation, D_5 is ON and other diodes are OFF. Therefore, one diode from each phase is ON and therefore, sum of phases current is zero (Figure 5). The line current in this time interval follows in the Equation (14).

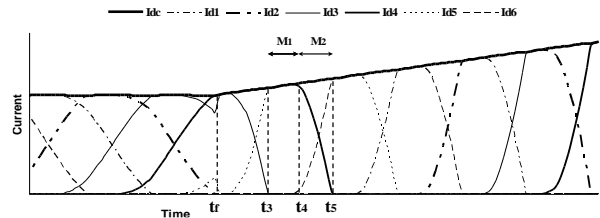


Figure 4. DC current and diodes currents in the fault condition

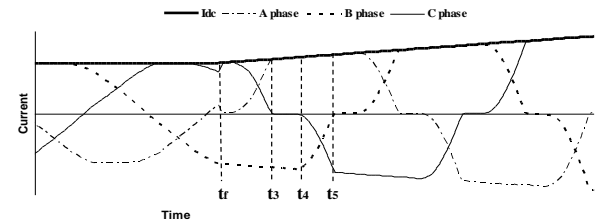


Figure 5. Line current and DC current in the fault condition

$$i_A(t) = e^{-\frac{r}{L}(t-t_4)} (I_4 - \frac{V_m}{z} \sin(\omega t_4 - \varphi) + \frac{V_D}{r}) + \frac{V_m}{z} \sin(\omega t - \varphi) - \frac{V_D}{r} \quad (14)$$

where, $I_4 = i_A(t_4)$. Similar to the previous mode, DC current follows the current of phase A relation. The currents of phase B and C can be driven from Equation (14) with corresponding phase shift. This manner of variation will be repetitive for next steps in the fault condition.

IV. TRANSIENT STABILITY ANALYSIS USING THE PROPOSED FCL

In this section, it will be shown that the proposed FCL can improve the transient stability of power system by absorbing the energy during fault and restoring the voltage of connected bus. It is possible to model the FCL by a resistor during the fault, but it should be considered that this resistor is not an ordinary resistor and should be calculated. For this calculation, we used the relation of energy stored in SMES magnet during the fault as follow:

$$w = \frac{1}{2} L_{SMES} I_{SMES}^2 \quad (15)$$

where, w is the energy stored in SMES magnet during the fault and I_{SMES} is the SMES magnet's current during the fault and can be written as Equation (16), approximately.

$$I_{SMES} = I_{max} + \frac{V_{dc}}{L_{SMES}} t \quad (16)$$

where, V_{dc} is the DC side voltage rectified by the diode bridge. So, the instantaneous power of SMES magnet can be concluded as follow:

$$P_{dc} = \frac{dw}{dt} = V_{dc} I_{max} + \frac{V_{dc}^2}{L_{SMES}} t \quad (17)$$

Considering Equation (17) and fault duration equal to t_f , average of active power absorbed by SMES magnet will be as Equation (18).

$$P_{dc,ave} = V_{dc} I_{max} + \frac{V_{dc}^2}{2L_{SMES}} t_f \quad (18)$$

Finally, considering the fact that the AC side and DC side active powers are equal and V_{dc} is equal to:

$$V_{dc} = \frac{6}{\pi} \sin\left(\frac{\pi}{3}\right) V_m \quad (19)$$

where, R_{fcl} (the model of proposed FCL during the fault in its ac side) can be concluded as Equation (20).

$$R_{fcl} = \frac{\pi V_m}{2\sqrt{3}(I_{max} + \frac{3\sqrt{3}V_m}{2\pi L_{smes}} t_f)} \quad (20)$$

It is important to note that this resistor has minimum and maximum limits as follows:

$$R_{fcl} \rightarrow \begin{cases} 0 & L_{SMES} = 0 \\ \frac{\pi V_m}{2\sqrt{3}I_{max}} & L_{SMES} \rightarrow \infty \end{cases} \quad (21)$$

Considering Equations (20), (21) and (24), larger value of L_{SMES} will lead to larger value of R_{fcl} and consequently better limitation of fault current and better enhancement of transient stability. However, large value of L_{SMES} will increase the design and construction difficulties and costs. Therefore, the value of L_{SMES} should be selected considering the maximum acceptable fault current. In other words, the maximum line current and minimum time in which the circuit breakers can open the line should be determined and then the value of L_{SMES} should be calculated by using Equation (16).

To show the effectiveness of the proposed FCL, Sum of the Maximum Oscillation (SMO) of all generators has been considered as a criterion for the stable power system

with and without the proposed FCL. Therefore, for the unstable power system, without the proposed FCL, the mentioned criterion will be infinite. Considering Figure 6, the maximum oscillation of a generator can be written as follow:

$$\Delta\omega_i = \omega_{max,i} - \omega_{min,i} \quad (22)$$

where, ω_i is angular frequency of generator i .

By using the proposed FCL, it will be shown in the simulation results that the sum of $\Delta\omega_i$ for all generators (i from 1 to 5) can be reduced, and as a result, transient stability of the power system will be improved. SMO for all generators can be expressed as Equation (23).

$$SMO = \sum_{i=1}^5 \Delta\omega_i \quad (23)$$

As mentioned above, SMO will be infinite for an unstable system. However, If SMO criterion is decreased by using the proposed FCL, it can be concluded that the FCL improves the transient stability of the power system.

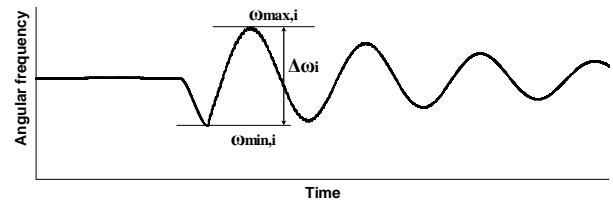


Figure 6. Schematic oscillation of a generator after fault

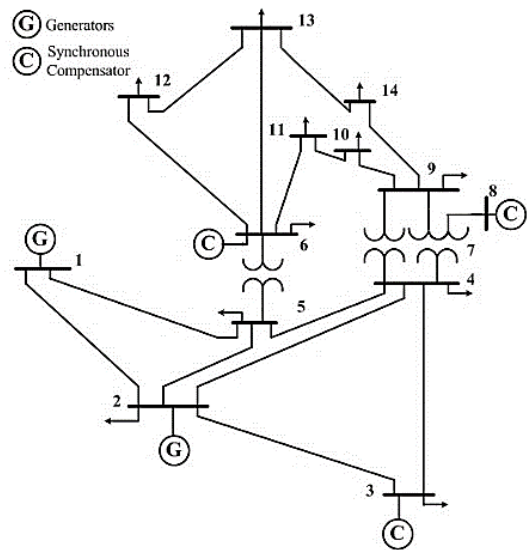


Figure 7. IEEE standard 14-bus power system

V. SIMULATION RESULTS

Simulations using EMTDC/PSCAD software are performed on Figure 7. Considering the history of measurements on system, it is assumed that the line between buses 7 and 9 is more supposed to short circuit faults. To study the performance of proposed FCL on current limitation and transient stability improvement, a three-phase to ground fault is considered at $t = 6$ sec. with the duration of 0.2 sec. (10 cycles of power frequency) in this line. In this simulation, value of L_{SMES} is calculated 0.48 H considering Equation (17) in section IV. Two sets of the proposed FCL are installed at two end of line 7-9.

Figure 8 shows the fault current without using the proposed FCL. In addition, Figure 9 shows the line 7-9 current from the bus 7 side. The current, which is flowed from bus 9 to the faulted point, is similar to Figure 9. Considering these figures, line current is increased extremely during the fault, which may cause the instability of generators. Figure 10 shows the generator 1 and 2 angular frequency in such condition. This figure shows that the synchronous generators angular frequencies start to increase uncontrollably and become unstable.

To show effect of fault on synchronous compensators, their angular frequencies are shown in Figure 11. According to this figure, during the fault, the lines resistance because of high short circuit currents that causes a decrement on their angular frequency absorbs synchronous compensators kinetic energy. After fault removal, they start to oscillate around the system base frequency and return to their normal state. Note that since the synchronous compensators do not provide active power for the system, they will be unstable in short circuit faults. However, after instability of generators and power system interruption, synchronous compensators speed declines to zero.

Moreover, the fault causes deep voltage sag on system buses. This voltage sag is more critical on buses, which are connected to the faulty line. Buses 7 and 9 voltages during the fault are shown in Figures 12 and 13, respectively. In general, instability of the generators is obvious from maintained figures.

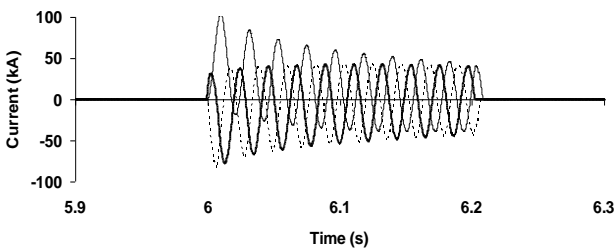


Figure 8. Three-phase fault current without using FCL

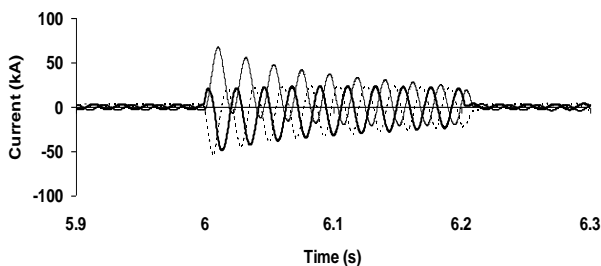


Figure 9. Fault current from bus 7 to the faulted point without using FCL

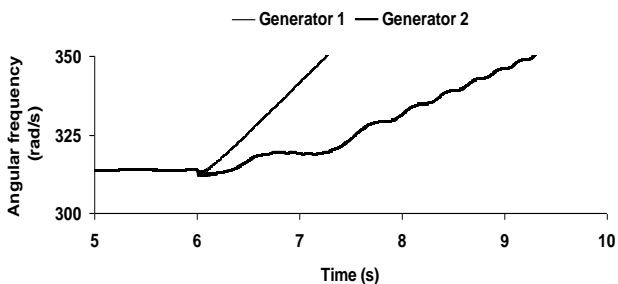


Figure 10. Gen. 1 and 2 angular frequency after fault without using FCL

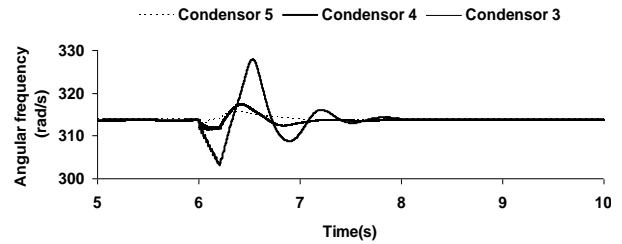


Figure 11. Angular frequency of synchronous compensators without using FCL

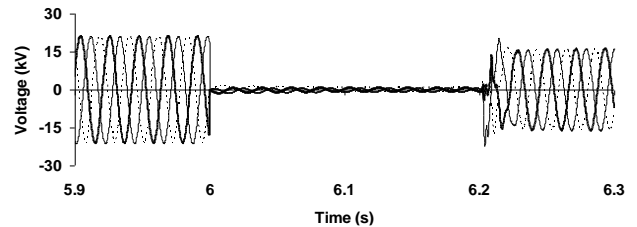


Figure 12. Voltage of bus 7 during the fault without using FCL

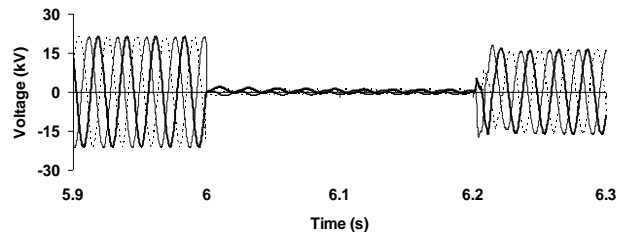


Figure 13. Voltage of bus 9 during the fault without using FCL

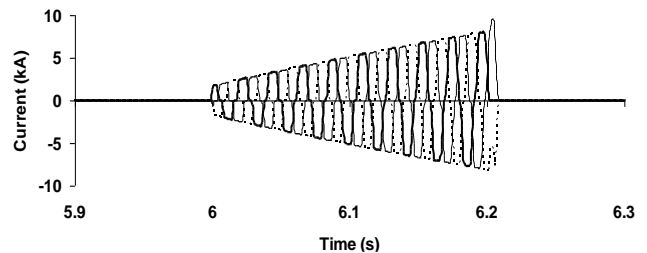


Figure 14. Fault current by using the proposed FCL

By using the proposed FCL and considering the SMES magnet's value equal to 0.48 H fault current is limited as shown in Figure 14. This leads to limitation of current flowed from the system to the faulted point. For instance, the fault current from bus 7 is shown in Figure 15. This effective limitation of fault current helps the generators to maintain their stability (Figure 16). In addition, as shown in this figure, the synchronous compensators experience very small deviation from the base frequency.

Figures 17 and 18 are shows voltage of bus 7 and 9 during the fault situation in presence of the proposed FCL. According to these two figures, voltages of these buses are restored properly. Because of these figures, using FCL prevents the instability of generators and improves the transient stability of whole system.

In addition, the SMO index, voltage sag prevention, and current limiting results in fault condition for the proposed SMES-based FCL are presented in Table 1. The SMO index is calculated using Equation (23). To study the voltage sag prevention capability of proposed FCL, average of voltage sag on all power system buses are calculated as follow:

$$V_{sag}^{ave} = \frac{1}{14} \left\{ \sum_{k=1}^{14} \left[\frac{(V_k^N - V_k^F)}{V_k^N} \right] \right\} \quad (24)$$

In addition, Equation (25) assesses current limiting performance of FCL.

$$I_F = I_{max}^F / I_{max}^N \quad (25)$$

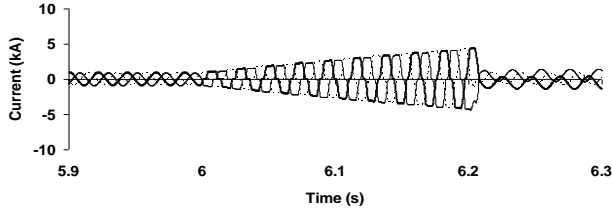


Figure 15. Current of bus 7 to the faulted point with the proposed FCL

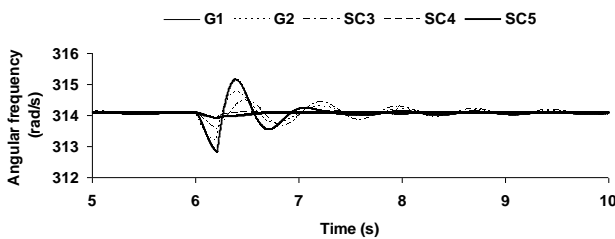


Figure 16. Generators 1 and 2 and synchronous compensators angular frequency with the proposed FCL

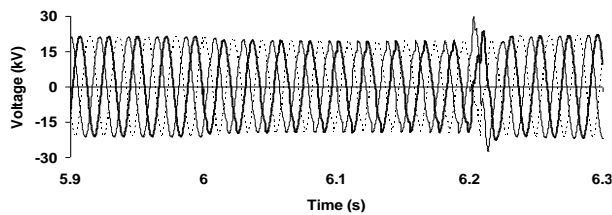


Figure 17. Voltage of bus 7 during fault with the proposed FCL

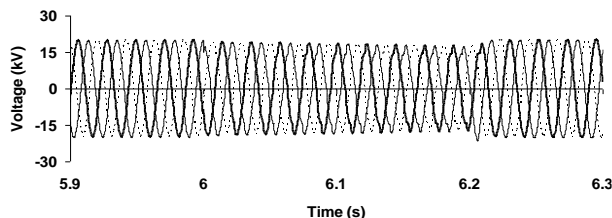


Figure 18. Voltage of bus 9 during fault with the proposed FCL

As pointed previously, without using FCL, system becomes unstable and *SMO* index will be infinite, while by using FCL it is decreased to 4.0197 (rad/s). Average voltage sag is reduced from 56.28 % in no FCL condition to 5.71 % with using the proposed FCL. Improvement of voltage profile during the fault is obvious from these results. In addition, current limiting capability of FCL is presented in Table 1. The fault current is limited to about 4.5 pu, while without using FCL, the magnitude of fault current was 3 to 5 times greater than its normal value.

Table 1. Values of *SMO*, voltage sag and fault current

	Without FCL	With FCL
<i>SMO</i> (rad/s)	Inf.	4.0197
Average Voltage Sag (%)	56.28	5.71
Current Limitation	Line 7 (pu)	22.4667
	Line 9 (pu)	12.4367

VI. CONCLUSIONS

In this paper, enhancement of power system's transient stability by using a SMES-based FCL is proposed. The proposed SMES-based FCL can improve the transient stability by two ways. Firstly, by preventing the voltage sag in connected bus during the fault and secondly by absorbing the acceleration power of generators in the fault interval and storing it in SMES magnet. By this manner, the synchronous generators can keep their stability after the short circuit faults.

Sum of maximum oscillations (*SMO*) of generators angular frequency and average of voltage sag on system buses are considered as indices to evaluate the transient stability and voltage profile improvement capability of the proposed FCL. In general, analytical analysis and simulation results using EMTDC/PSCAD software in standard IEEE 14-bus system show that the proposed FCL has acceptable performance in transient stability enhancement and voltage profile improvement in addition to fault current limiting.

REFERENCES

- [1] M. Jafari, S.B. Naderi, M. Tarafdar Hagh, M. Abapour, S.H. Hosseini, "Voltage Sag Compensation of Point of Common Coupling (PCC) Using Fault Current Limiter", IEEE Transactions on Power Delivery, Vol. 26, No. 4, pp. 2638-2646, October 2011.
- [2] M. Sedighzadeh, B. Minoie, M. Sarvi, "Power System Stability Enhancement Using a NSPSO Designed UPFC Damping Controller", International Journal on Technical and Physical Problems of Engineering (IJTPE), Issue 14, Vol. 5, No. 1, pp. 1-8, March 2013.
- [4] S.B. Naderi, M. Jafari, M. Tarafdar Hagh, "Parallel Resonance Type Fault Current Limiter", IEEE Trans. Ind. Electron., Vol. 60, No. 7, pp. 2538-2546, July 2013.
- [5] M. Mohammadi, N. Javidsht, M. Parhoodeh, "Stability Enhancement of DFIG Wind Turbines by Parameters Tuning of FACTS Devices", International Journal on Technical and Physical Problems of Engineering (IJTPE), Issue 14, Vol. 5, No. 1, pp. 82-88, March 2013.
- [6] Y. Lin, L.L. Zhen, K.P. Juengst, "Application Studies of Superconducting Fault Current Limiters in Electric Power Systems", IEEE Trans. Appl. Superconducting, Vol. 12, No. 1, March 2002.
- [7] M. Tarafdar-Hagh, M. Abapour, "Non-Superconducting Fault Current Limiter with Controlling the Magnitudes of Fault Currents", IEEE Trans. Power Electron., Vol. 24, No. 3, March 2009.
- [8] H. Ohsaki, M. Sekino, S. Nonaka, "Characteristics of Resistive Fault Current Limiting Elements Using YBCO Superconducting Thin Film with Meander-Shaped Metal Layer", IEEE Trans. Appl. Supercond., Vol. 19, No. 3, pp. 1818-1822, June 2009.
- [9] V. Sokolovsky, V. Meerovich, I. Vajda, V. Beilin, "Superconducting FCL - Design and Application", IEEE Trans. Appl. Supercond., Vol. 14, No. 3, pp. 1990-2000, September 2004.
- [10] S.H. Lim, H.S. Choi, D.Ch. Chung, Y.H. Jeong, Y.H. Han, T.H. Sung, B.S. Han, "Fault Current Limiting

Characteristics of Resistive Type SFCL Using A Transformer", IEEE Trans. Appl. Supercond., Vol. 15, No. 2, pp. 2055-2058, June 2005.

[11] T. Hoshino, K.M. Salim, M. Nishikawa, I. Muta, T. Nakamura, "DC Reactor Effect on Bridge Type Superconducting Fault Current Limiter During Load Increasing", IEEE Trans. Appl. Supercond., Vol. 11, No. 1, pp. 1944-1947, March 2001.

[12] M. Tarafdar-Hagh, M. Abapour, "Non-Superconducting Fault Current Limiters", Euro. Trans. Electr. Power, Vol. 19, No. 5, pp. 669-682, July 2009.

[13] G.T. Son, H.J. Lee, S.Y. Lee, J.W. Park, "A Study on the Direct Stability Analysis of Multi-Machine Power System with Resistive SFCL", IEEE Trans. Appl. Superconduct., Vol. 22, No. 3, Article No. 5602304, June 2012.

[14] I. Ngamroo, S. Vachirasricirikul, "Coordinated Control of Optimized SFCL and SMES for Improvement of Power System Transient Stability", IEEE Trans. Appl. Superconduct., Vol. 22, No. 3, Article No. 5600805, June 2012.

[15] M. Ferrier, "Energy Storage in a Superconducting Winding in Low Temperature and Electric Power", Pergamon Press, pp. 425-432, 1970.

[16] J.D. Rogers, "30-MJ SMES System for Electric Utility Transmission Stabilization", Proc. IEEE, Vol. 71, pp. 1009-1107, 1983.

[17] R.J. Loyd, S.M. Schoenung, T. Nakamura, W. Hassenzahl, J.D. Rogers, J.R. Hrcell, D.W. Lieurance, M.A. Hilal, "Design Advances in Superconducting Magnetic Energy Storage for Electric Utility Load Leveling", IEEE Trans. Mag., Vol. 23, pp. 1323-1330, 1987.

[18] F. Fattahi, N.M. Tabatabaei, N. Taghizadegan, "Damping of Oscillations of Azerbaijan Electrical Network by SMES System and Fuzzy Controller", International Journal on Technical and Physical Problems of Engineering (IJTPE), Issue 2, Vol. 2, No. 1, pp. 11-14, March 2010.

[19] A. Jalili, H. Shayeghi, N.M. Tabatabaei, "Fuzzy PID Controller Based on LFC in the Deregulated Power System Including SMES", International Journal on Technical and Physical Problems of Engineering (IJTPE), Issue 8, Vol. 3, No.3 , pp. 38-47, September 2011.

[20] E.R. Lee, S. Lee, C. Lee, H.J. Suh, D.K. Bae, H.M. Kim, Y.S. Yoon, T.K. Ko, "Test of DC Reactor Type Fault Current Limiter Using SMES Magnet for Optimal Design", IEEE Trans. Appl. Supercond., Vol. 12, No. 2, pp. 850-853, March 2002.

[21] I. Ngamroo, S. Vachirasricirikul, "Optimized SFCL and SMES Units for Multi-Machine Transient Stabilization Based on Kinetic Energy Control", IEEE Trans. Appl. Superconduct., Vol. 23, No. 3, Article No. 5000309, June 2013.

[22] M. Jafari, A. Vafamehr, M.R. Alizadeh Pahlavani, "Transient Stability Enhancement Using SMES-Based Fault Current Limiter", International Review of Automatic Control (IREACO), Vol. 5, No. 6, pp. 749-756, November 2012.

[23] G. Didier, J. Leveque, A. Rezzoug, "A Novel Approach to Determine the Optimal Location of SFCL in Electric Power Grid to Improve Power System Stability", IEEE Trans. Power Sys., Vol. 28, No. 2, pp. 978-984, May 2013.

[24] Y. Shirai, K. Furushiba, Y. Shouno, M. Shiotsu, T. Nitta, "Improvement of Power System Stability by Use of Superconducting Fault Current Limiter with ZnO Device and Resistor in Parallel", IEEE Trans. Appl. Supercond., Vol. 18, No. 2, pp. 680-683, June 2008.

[25] K. Furushiba, T. Yoshii, Y. Shirai, K. Fushiki, J. Baba T. Nitta, "Power System Characteristics of the SCFCL in Parallel with A Resistor in Series with A ZnO Device", IEEE Trans. Appl. Supercond., Vol. 17, No. 2, pp. 1915-1918, June 2007.

[26] B.Ch. Sung, D.K. Park, J.W. Park, T.K. Ko, "Study on a Series Resistive SFCL to Improve Power System Transient Stability - Modeling, Simulation and Experimental Verification", IEEE Trans. Ind. Electron., Vol. 56, No. 7, pp. 2412-2419, July 2009.

[27] B.Ch. Sung, J.W. Park, "Optimal Parameter Selection of Resistive SFCL Applied to A Power System Using Eigenvalue Analysis", IEEE Trans. Appl. Supercond., Vol. 20, No. 3, pp. 1147-1150, June 2010.

BIOGRAPHIES



Mehdi Jafari was born in Ahar, Iran. He received the B.Sc. and M.Sc. degrees in Power Engineering from University of Tabriz, Tabriz, Iran, in 2008 and 2011, respectively. He is currently with the Ahar Branch, Islamic Azad University, Ahar, Iran. His current research interests include

fault current limiters, power quality and power system transient.



Mohammad Reza Alizadeh Pahlavani received the Ph.D. degree in Electrical Engineering from Iran University of Science and Technology, Tehran, Iran in 2009. Currently he is in Department of Electrical Engineering, Malek Ashtar University of Technology, Tehran,

Iran. He is the author of more than 110 ISI transactions journals, international, and national conference papers in the field of electromagnetic systems, electrical machines, power electronic, FACTS and pulsed power.